Dynamic modelling and optimal sizing of industrial fire-tube boilers for various demand profiles

Marco Tognoli, Behzad Najafi *, Fabio Rinaldi

Dipartimento di Energia, Politecnico di Milano, Via Lambruschini 4, 20156 Milano, Italy

In the present paper, a detailed dynamic model of an industrial fire-tube boiler is first developed and five different geometrical configurations, each of which corresponds to a boiler model, are considered. Next, a PID controller is implemented and tuned for each configuration aiming at controlling the steam pressure, while addressing a demand with a variable flow rate. The operation of the developed boiler models, while providing four different steam demand profiles, are next simulated. The resulting cumulative average efficiency along with the cumulative pressure deviations and minimum and maximum pressure levels, which are achieved in each simulation, are then determined. The obtained results provide practical infor-mation regarding the trade-off between the size of the boiler and its corresponding performance and con-trollability. As an instance, the obtained results demonstrated that utilizing a boiler with the heat transfer surface of 36.76 m^2 instead of one with the corresponding surface of 56.55 m^2, in the worst-case scenario, leads to less than 2% of reduction in the efficiency and a negligible increment in the amplitude of pressure deviations. However, the former boiler is considerably smaller than the latter one and the mentioned choice can result in a significant saving in the required initial investment. Detailed information regarding the resulting pressure deviations has also been provided in order to facilitate verifying the consistency of the variations in each boiler's supplied steam pressure with the corresponding acceptable range specified by the customer. Therefore, the provided results offer useful insights about the possible saving opportu-nities for small-medium scale industries, specifically in Italy, which are commonly employing oversized boilers with an On/Off control systems.

Keywords: Fire-tube boiler, Dynamic modelling, Finite element method, PID tuning, optimal sizing

H I G H L I G H T S

- A detailed FEM based dynamic model for a fire-tube boiler is developed.
- Five configurations, representing different boiler models, are taken into account.
- A PID controller is tuned for each configuration.
- The performance of boilers, while addressing four demand profiles, is investigated.
- Cumulative efficiency and pressure deviation in each simulation are determined.

1. Introduction

Fire-tube boilers are widely used as low-medium pressure steam sources thanks to their numerous advantages including the feasibility of being fed by several types of fuels [1]. In these types of boilers, the combustion process takes place in the suited chamber and the generated flue gases then go through tube passes, in which heat is transferred to the water filling the shell side. The large mass of water stored in the shell provides these types of boilers with a notable thermal inertia. Accordingly, the behaviour of these units, specifically while addressing an intermittent load, is far from the steady-state condition. Hence, in order to accurately simulate the performance of these boilers, their corresponding dynamic behaviour should be simulated. Most of the previous studies on dynamic modelling of boilers have been focused on water-tube units units [2–11] and very few works have been conducted on fire-tube ones. The studies on water-tube boilers are mainly dedicated to specific aspects of gas/fire side [12] (owing

Article history:
Received 3 September 2017
Revised 2 December 2017
Accepted 23 December 2017
Available online 26 December 2017

* Corresponding author.
E-mail addresses: marco3.tognoli@mail.polimi.it (M. Tognoli), behzad.najafi@polimi.it (B. Najafi), fabio.rinaldi@polimi.it (F. Rinaldi).

Published Journal Article available at https://doi.org/10.1016/j.applthermaleng.2017.12.082

Nomenclature

A	heat exchange surface [m^2]
A/F_{st}	stoichiometric air/fuel ratio [kg_{air}/kg_{fuel}]
A/F_{real}	actual air/fuel ratio [kg_{air}/kg_{fuel}]
C	fuel carbon content [w%]
c_P	isobaric specific heat $\left[\frac{kJ}{°C \cdot kg}\right]$
c_V	isocoric specific heat $\left[\frac{kJ}{°C \cdot kg}\right]$
CTM	global specific heat of metal active parts [J/°C]
$\bar{e}$	average wall tubes thickness [mm]
AE	air excess [w%]
$f(x)$	inherent characteristic of the control valve
h	specific enthalpy [kJ/kg]
$\bar{h}_{C,water}$	average liquid water convective heat transfer coefficient $\left[\frac{kJ}{m^2 \cdot s \cdot °C}\right]$
$\bar{k}_t$	average metal thermal conductivity of gas pass tubes $\left[\frac{kJ}{m^2 \cdot s \cdot °C}\right]$
K_{VS}	control valve flow coefficient [–]
LHV	lower heating value of fuel [MJ/kg]
l	boiler height or boiler diameter [m]
L	boiler length [m]
m	mass [kg]
$\dot{m}_{fuel}$	fuel flow rate [kg/s]
$\dot{m}_g$	flue gas mass flow rate [kg/s]
M	molecular weight [kg/kmol]
M_s	simulation time intervals [–]
$n_{t,j}$	number of tubes in a gas pass section at given tube bank j [–]
P	pressure [*bar*]
$\dot{Q}_{g\rightarrow w}$	heat transferred from hot flue gases to water shell [kW t]
$\sum_j \dot{q}_{j,water}$	heat gained by water [kW t]
R_g	perfect gas constant $\left[\frac{m^3 \ Pa}{mol \ K}\right]$
$R_{ext,H}$	tube external radius [m]
t	time [s]
T	temperature [°C]
V	volume [m^3]
v_g	gas velocity [m/s]
v	specific volume [m^3/kg]
x	valve open fraction [–]
x_V	vapour quality [–]
Y	fuel heat release fraction along axial distance [MJ/MJ_{tot}]

Greek symbols

α	efficiency factor of heat transfer due to convection and radiation [–]
ε	emissivity [–]
$\bar{\lambda}$	average water latent heat [kJ/kg]
η	efficiency parameter [–]
ρ	density [kg/m^3]

Subscripts

H_2O	water
$+$	upper zone of the boiler chamber, vapour zone
$-$	lower zone of the boiler chamber, liquid zone
amb	ambient conditions around the boiler
chim	chimney section
cons	quantity consumed in a chemical process
i	furnace and tubes element
in	inlet
f	feedwater
g	flue gas
gen	quantity generated in a chemical process
j	gas pass number
p	purge water
wall	tube wall
out	outlet
sum	section downstream of the steam control valve to the enduser
t	metal tube
v	vapour

to the importance of heat flux characteristics and temperature distribution [13]) or water/steam sides [9,14,15], along with the control strategy on the water level [16,17]. Sørensen et al. [18] simulated the dynamic behaviour of the fire-tube boilers employing a modular model consisting of several sub-models, each of which represents a different zone in the boiler. Each sub-model was developed utilizing differential algebraic equations while considering the corresponding physical principles. Huang and Ko [19] proposed a nonlinear time variant dynamic model for the fire-tube boiler based on the corresponding transport phenomena. The model was validated thanks to the results of experimental investigations and various parameters were also directly obtained from the obtained test results. They demonstrated that their developed semi-empirical model is able to accurately predict the dynamic response and the resulting performance of fire-tube boilers over a wide range of operating conditions. Rusinowski and Stanek [20] developed a neural network based model for simulating the dynamic behaviour of boilers. Their developed data-driven model relates boiler's operational parameters to the flue gas losses and losses due to unburned combustibles. The machine-learning based approach, as a data-driven methodology, is considered to be a promising modelling strategy when sufficient geometrical information or material properties for developing a physical model is not accessible, although it can be prone to notable accuracies in extrapolation condition [21].

Some of the works focused on fire-tube boilers, have been conducted employing CFD (Computer Fluid Dynamics) models [22–26]. Apparently utilizing this approach facilitates accurate simulation of the turbulent fluid flow in the flue gas side, the radiative heat transfer mechanism along the gas passes, and the convection interactions with combustion chamber's walls. Nevertheless, employing CFD models results in a considerable computational cost [27] and thus is not an appropriate choice for dynamic modelling and determination of optimal control strategy for the boilers, which requires several repetitive simulations.

Gutiérrez Ortiz [28] provided a comprehensive dynamic modelling methodology for fire-tube boilers introducing both a more complex approach (utilizing finite element methods) and a simplified model. This methodology considers all of the key physical phenomena, taking place in the boiler, and it results in a notably lower computational cost, compared to the CFD models, while providing an acceptable accuracy.

In small/medium scale industries, specifically in Italy, similar to several other small-scale heat and power generation units [29,30], the employed boilers are commonly oversized and many of them are controlled by On/Off controllers. Thus, considering the dynamic behaviour of the boiler in the corresponding sizing procedure, while taking into account the demand profile of the customer, can lead to significant savings in the required capital cost. Furthermore, similar to many other thermal components and

power generation units [31,32], there is a trade-off between the energetic efficiency of boilers and their corresponding required investment. Hence, determining the efficiency of different boiler models, while meeting the demand profile of the customer, can help the decision makers to choose the optimal size of the boiler considering the customer's specifications and the corresponding key economic criteria.

Accordingly, in the present study, a dynamic model of a fire-tube boiler, employing the more complex approach proposed in the Gutiérrez Ortiz's methodology [28], is developed. The developed model is based on mass and energy balances for both the water and the flue gas sides, in which a FEM (finite element method) based approach is utilized in order to accurately simulate the behaviour of the latter side. Next, five geometrical configurations, representing different models of boilers designed by our industrial partner (ICI Caldaie S.p.A), are considered. A PID based control strategy is next implemented and the plant linearization (in the nominal condition) and PID tuning is carried out for all of the considered configurations. Afterwards, four different steam demand profiles, which represent a wide range of customer requirements, are considered and the operation of the considered boiler models, while addressing the mentioned profiles, is simulated. In order to evaluate the performance and controllability of each boiler while addressing the considered profiles, the corresponding cumulative average efficiency along with the cumulative pressure deviations and the minimum and maximum pressure levels are determined.

The obtained results, for a specific profile, demonstrate the effect of choosing a smaller boiler on the efficiency and the pressure deviation range of the supplied steam. Thus, practical information regarding the possible savings, while meeting the customer requirement, is provided. In order to provide more detailed information about the amplitude and duration of pressure deviation peaks, pressure variation diagrams of boilers, while addressing different profiles, are also included.

2. Unit description

Fig. 1 demonstrates a schematic view of the fire-tube boiler, which is simulated in the present paper. As can be seen in this figure, the premixed combustion is taking place in the combustion chamber and the generated flue gases then enter the tube passes. Water is instead entering the shell side where it is heated up and then evaporated through exchanging heat with the flue gases passing through combustion chamber and the gas passes. The generated steam eventually leaves the boiler through the steam extraction valve.

3. Model description

The developed dynamic model constitutes two main separate sections of flue gas side and the evaporating shell, which are integrated employing the energy balance. The main assumptions and the implemented governing equations of these main parts of the model are given in the following sections:

3.1. Flue gas side

In order to simulate the flue gas side, it is assumed that the air and fuel are ideally premixed and the premixed combustion is taking place in the combustion chamber. Air-to-fuel mass ratio is assumed to be constant and set thanks to the desired outlet oxygen concentration. Since the combustion reactions are very fast, and considering the elevated temperatures in the combustion chamber, it is assumed that the reactant are instantaneously converted into products; thus the combustion reaction kinetics are ignored. The generated flue gas is considered to be an ideal gas with the composition, which is determined considering complete combustion.

Regarding the heat transfer phenomena, the radial component of the radiative heat transfer is considered while the axial one is neglected. The radiation heat transfer is thus assumed to take place between an ideal grey emitting gas body and an isotropic and grey wall surface. Furthermore, in order to accurately simulate the radiative heat transfer in the flue gas side, the gas passes are discretised. The architecture of the employed finite element method (FEM) based strategy is represented in Fig. 2. In the present model, 100 elements have been employed for the furnace (N_F = 100) and 20 elements for each gas pass ($N_j = 20$). The mentioned numbers of elements have been determined to be optimal solutions

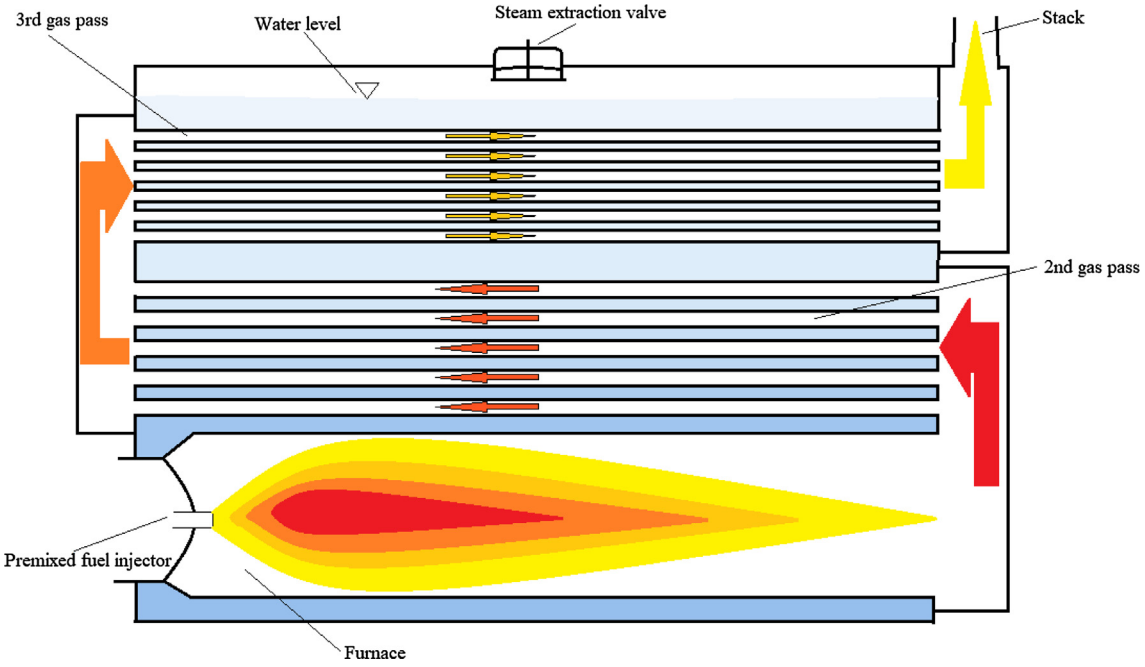

Fig. 1. A schematic diagram of the Fire-tube boiler.

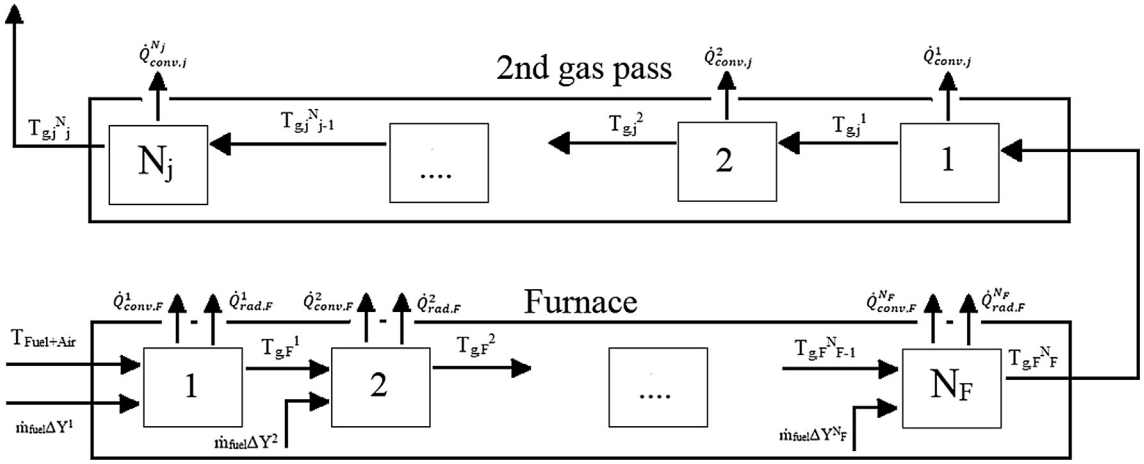

Fig. 2. Structure of the developed FEM.

considering the trade-off between the approximation error and the calculation cost.

Wall temperature of combustion chamber as well as other gas passes is assumed to be constant and uniform along tubes length. The later assumption is reasonable due to the elevated convective heat transfer coefficient at the water side [33].

3.1.1. Combustion chamber

The mass balance equation for each cylindrical element, obtained from discretization procedure, is as follows:

$$\frac{d}{dt}m_k^i = m_{k,in}^i - m_{k,out}^i - m_{k,cons}^i + m_{k,gen}^i = m_{k,in}^{i-1} - m_{k,out}^i - m_{k,cons}^i + m_{k,gen}^i \quad (1)$$

Eq. (1) is valid for each element i in every component k. The mass balance for this system does not account for the generated mass, as $\frac{d}{dt}m_k^i = 0$.

For the given system, the mass of flue gases is clearly the sum of that of air and the fuel. Heat is released by fuel combustion and the heat flux is determined by the fuel lower heating value and fuel flow rate ($\dot{m}_{fuel} \cdot LHV$). The flame propagates along the chamber axis and it is designed to occupy almost the entire combustion chamber length. The heat release distribution is function of the fractional length along the entire distance covered by the flame, the heat release rate follows an exponential type curve described by:

$$Y = 1 - \exp\left[-4.6\left(\frac{x}{L_F}\right)\right] \quad (2)$$

Moreover, the equation can be expressed in terms of discrete section i by N_F and the fraction of the heat release rate at element i can consequently be expressed as:

$$\Delta Y_i = \exp\left[-4.6\left(\frac{i-1}{N_F}\right)\right] - \exp\left[-4.6\left(\frac{i}{N_F}\right)\right] \quad (3)$$

The Dittus-Boelter correlation for fluids in turbulent regime [34], is employed for simulating the convective heat transfer mechanism. The model proposed by Hottel and Sarofim [35] is instead utilized for simulating the radiative heat transfer mechanism between the grey flue gases and grey walls. All the surfaces are assumed to be perfect grey bodies; hence, for each element i of the furnace:

$$\frac{d}{dt}(\rho_{g,H}VC_{v\,g,F}T_{g,F}^i) = \dot{m}_{fuel}LHV\Delta Y_i + \dot{m}_g\bar{c}_{P,g,F}(T_{g,F}^{i-1} - T_{g,F}^i) - \dot{q}_{rad,F}^i - \dot{q}_{conv,F}^i \quad (4)$$

where the convective and radiative heat transfer terms can be determined by:

$$\dot{q}_{conv,F}^i = \bar{h}_{c,F}\frac{\pi L_F}{N_F}(T_{g,F}^i - T_{wall,F}) \quad (5)$$

$$\dot{q}_{rad,F}^i = \frac{2\pi R_{int,F}L_F}{N_F}\sigma\frac{\varepsilon_{wall,F}+1}{2}\varepsilon_{g,F}(T_{g,F}^{i4} - T_{wall,F}^4) \quad (6)$$

where

$$\bar{h}_{c,F} = 0.023k_{g,F}Re^{0.8}Pr^{0.4} \quad (7)$$

The formation of soot has been neglected in the present model. Regarding the emissivity of fuel, the correlations provided by Hottel [36] are employed.

In order to take into account the heat exchange between the gases in the combustion chamber and the water in the shell side, the following correlations are employed:

$$m_{t,F}c_{P_{t_F}}\frac{d}{dt}T_{wall,F} = \sum_{i=1}^{N_F}(\dot{q}_{rad,F}^i + \dot{q}_{conv,F}^i) - \dot{q}_{F,water} \quad (8)$$

where

$$\dot{q}_{F,water} = \frac{2\pi R_{ext,F}L_F}{\frac{R_{ext,F}}{k_{t,F}}ln\left(\frac{1}{1-\frac{e_F}{R_{ext,F}}}\right) + \frac{1}{h_{c,water}}}(T_{wall,F} - T_{water}) \quad (9)$$

where $\dot{q}_{F,water}$ represent the heat flux effectively transferred to the water side which is calculated at the external furnace side.

3.1.2. Gas passes

Energy balance equation for the following gas passes is specified for j tube bank ($j = 2,3,4$) considering the number of tubes per tube bank ($n_{t,j}$):

$$\frac{1}{n_{t,j}}\frac{d}{dt}(V_jc_{v_{g,j}}\rho_{g,j}T_{g,j}^i) = \frac{\dot{m}_g}{n_{t,j}}\bar{c}_{P,g}(T_g^{i-1} - T_g^i) - \dot{q}_{conv,j}^i \quad (10)$$

Each tube of every gas pass it is discretized into N_j elements where:

$$\dot{q}_{conv,j}^i = \bar{h}_{c,j}\frac{\pi L_j}{N_j}(T_{g,j}^i - T_{wall,j}) \quad (11)$$

$\bar{h}_{c,j}$ is expressed in [W/m K]. In order to model the heat exchange between the flue gases, passing through the gas passes, and the water in the shell side, the following relations are utilized:

$$m_{t,j}c_{P_{t_j}}\frac{d}{dt}T_{wall,j} = n_{t,j}\sum_{i=1}^{N_j}[(\dot{q}^i_{rad,j} + \dot{q}^i_{conv,j}) - \dot{q}_{j,water}] \tag{12}$$

$$\dot{q}_{j,water} = \frac{2\pi n_{t,j}R_{ext,j}L_j}{\frac{R_{ext,j}}{k_{t,j}}ln\left(\frac{1}{1-\frac{e_j}{R_{ext,j}}}\right) + \frac{1}{h_{c,water}}}(T_{wall,j} - T_{water}) \tag{13}$$

3.2. Water/vapour side

In order to simulate the water-vapour (shell) side, three main mass flow rates, including the ones corresponding to the supplied feedwater, the extracted steam, and the purge should be taken into account. The main incoming stream is the feedwater flow rate ($\dot{m}_f$) that is supplied to the drum boiler chamber at a certain temperature (T_f) by a centrifugal pump. The main outgoing mass flow rate is instead the extracted steam flow rate ($\dot{m}_v$) which leaves the shell through a mechanically controlled valve. The last one refers to the purge mass flow rate ($\dot{m}_p$), which is the saturated water extracted from the bottom of boiler shell in order to reduce the rising concentration of the mineral deposit. The later flow is managed by an external control device and can be modelled as an intermittent flow over time.

The boiler shell can be considered to be made up of two separated zones: the lower zone, which is filled with water and the upper zone or vapour zone, which fills the remaining free space. Heat exchange is designed to take place only between the bottom zone and tube banks, in order to prevent tubes from reaching critical temperature that may cause extensive thermal damage. Natural circulation with the cylindrical shells leads to continuous mixing, which leads to a relatively homogeneous distribution of temperature, pressure, and density in the bottom zone. A detailed scheme, which demonstrates the mentioned zones, is illustrated in Fig. 3.

The heat transfer taking place in the shell through the boiling process can be modelled employing the convective nucleate boiling mechanism in an enclosed surface. Cooper pool boiling correlation [37] is used in the present work in order to calculate boiling heat transfer coefficient at water tube banks side, while considering 1 μm boiling surface roughness. The following correlation is utilized:

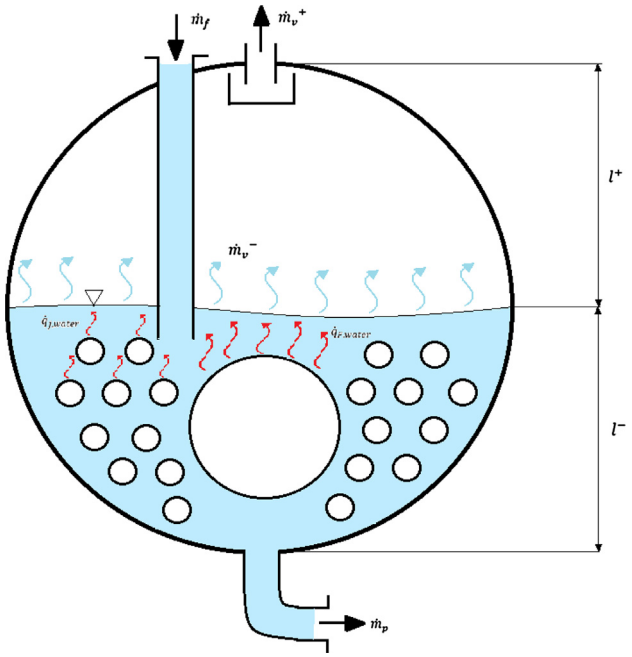

Fig. 3. Boiler cross section, description of upper/lower zones.

$$h_{nb} = 12.96Pr^{0.12} - [0.4343\ln(Pr)]^{-0.55}\left(\frac{Q}{A}\right)^{0.67} \tag{14}$$

where Q/A refers to the specific heat flow rate expressed in $[W/m^2]$. Cooper correlation is valid between 2 and 15bar in pressure range.

In the present study the water and vapour sides are considered to be at thermal equilibrium. In the following sections, the governing equations, employed for simulating each side, are provided.

3.2.1. Upper zone (+)/saturated steam

Considering the fact that the mass of the stored vapour has a negligible effect on the mass storage of the liquid water, it is reasonable to neglect the vapour mass storage. In other words, the vapour flow rate extracted from the valve can be considered to be equal to the vapour yield obtained from liquid water evaporation. Furthermore, considering the geometry of the boiler and the fraction of volume occupied by the vapour, vapour level variation can be expressed as:

$$\frac{dV^+}{dt} = 2RL\frac{dl^+}{dt} \tag{15}$$

The above-mentioned equation is based on the hypothesis that water level, although continuously variating, is close to the middle height of the shell.

3.2.2. Lower zone (−)/Saturated liquid water

Considering the mass balance for the liquid water zone:

$$\frac{d}{dt}(\rho^-V^-) \approx \rho^-\frac{d}{dt}V^- = \dot{m}_f - \dot{m}_p - \dot{m}_v^+ \tag{16}$$

Considering the total volume balance equation for incompressible liquid water, the sum of rate of variations of V^- and V^+ is zero. In order to determine the mass flow rate of the extracted steam, the general steam control valve equation is utilized, in which it is a function of pressure difference between the shell and the downstream side, valve open factor f_s (which has a linear behaviour), and the valve mass flow coefficient K_{VS}:

$$\dot{m}_v^+ = K_{VS}C^s f_s(x)\sqrt{(P^+ - P_{sum})\rho^+} \tag{17}$$

where C^s is a unit conversion factor. As was previously mentioned, the mass storage effect in the present model is entirely accounted for liquid water portion; this assumption is represented in the following correlation:

$$\rho V_{total} = \rho^-(T)V^-(l^+) + \rho^+(T)V^+(l^+) \approx \rho^-(T)V^-(l^+) \tag{18}$$

The main energy balance equation lead to:

$$\frac{d}{dt}T \cong \frac{1}{\rho V_{total}\bar{c}_V}[\dot{m}_f\bar{c}_{p_f}(T_f - T) - \dot{m}_v^+\bar{\lambda} + \dot{q}_{F,water} + \sum_{j=2}^{3,4}\dot{q}_{j,water}] \tag{19}$$

where the difference between the feedwater flow rate ($\dot{m}_f$) and the extracted steam flow rate ($\dot{m}_v^+$) corresponds to the purge water flow rate $\dot{m}_p$. The boiler first principle efficiency is consequently calculated as:

$$\eta_{boiler,I} = \frac{\sum_{j=1}^{j=M_s}(m_{v_j}^+h_{v_j}^+ - \mathrm{m}_{f_j}h_{f_j})}{\sum_{j=1}^{j=M_s}(\mathrm{m}_{fuel_j}\cdot LHV)} \tag{20}$$

where j corresponds to the simulation time interval ($j = 1$ to $j = M_s$ (end of simulation). The length of time intervals is kept constant (dt); hence, the generated mass of steam (at each time interval ($m_{v_j}^+$) is equal to the product of the corresponding steam generation

rate ($\dot{m}^{+}_{v_j}$) and the time interval (dt). The same point also holds for the provided mass of feedwater at each time interval (m_{f_j}) and the corresponding consumed mass of fuel (m_{fuel_j}). It is noteworthy that the validation of the represented model has already been presented in [28].

4. Control strategy

The considered fire-tube boiler has three main degrees of freedom to be controlled: the extracted steam flow rate, feedwater flow rate, and fuel/air flow rate. This flow rate of the extracted steam can be managed by the valve pressure difference and the valve position. Traditionally the valve position is not controlled; hence, keeping the internal pressure constant, the driving force is the downstream pressure at the user side. The remaining two degrees of freedom are managed by an active control unit where the feedwater flow rate is controlled by a level control system and the fuel/air flow rate is controlled by a PID controller.

The level control system for controlling the feedwater mass flow rate utilizes two level scopes which are installed inside the boiler at different water levels. These levels represent the minimum and the maximum allowed liquid water volumes considering the security measures. Accordingly, the on/off switch system activates the feedwater pump, at the nominal flow rate, as soon as the water level reach the minimum point and shuts it off as it reaches the maximum. This simple control strategy allows savings in capital investments while guaranteeing the required security.

On the other hand, The PID controller controls the fuel/air flow rate through a closed loop which aims at keeping the boiler pressure at a reference value. In order to minimize the deviations from the reference value, The PID control function should be tuned. In order to conduct the tuning procedure, the behaviour of the plant while receiving a range of inputs should be known. The latter, can be obtained either through conducting experimental tests, while operating at various operating conditions, or simulating the estimated behaviour of the plant employing the developed former. Apparently, conducting laboratory tests requires notable time and investment; thus employing a validated model to predict the performance of the plants in order to tune the PIC controller results in a significant economic benefit. Employing the developed dynamic model, PID tuning is conducted through the linearization technique. Plant linearization procedure derives the plant transfer function based on input and output variable(s) depending if the PID manage one or more degree of freedom. One common approach for linearizing non-linear systems is the feedback linearization control which is conducted through changing variables [38]. The mentioned approach has been utilized in the present study in order to linearize the plant and then tune the PID controller.

5. Results and discussions

Once the dynamic model of the plant is developed, different geometrical configurations, representing different boiler models, are taken into account. Table 1 represents the geometrical parameters of the five boiler models that are considered in the present study. It is noteworthy that a set of geometrical parameters including the furnace metal thickness (5 mm), 2nd gas pass tubes radius (25 mm), and 2nd gas pass tubes thickness (5 mm) have been kept constant in all of the configurations. Next, the plant linearization and PID tuning is carried out for all of the considered configurations.

Afterwards, four different steam request profiles (demonstrated in Fig. 4) with the duration of three hours, which represent a wide range of customer requirements, are taken into consideration. Profile No. 1 represents a typical manufacturing company with steady periods of production followed by periods corresponding to the standby state. Profile No. 2 instead represents a more recurrent trend with moderate variability minimizing the upper limit of extracted steam at 2500 kg/h. Profile No. 3 and No. 4 are designed with the same base period of 625 s, where the former represents a very limited range of variability. The latter one instead shows a wider amplitude in order to represent sudden requests and down time, which indeed is the most challenging demand profile to address. Table 2 represent the general operating conditions that are applied while simulating the system's behaviour while addressing these profiles.

The operation of different boiler models, while meeting the considered steam demand profiles, is then simulated. For each simulated boiler model and profile, the performance and the controllability of the unit are evaluated. Cumulative average boiler efficiency, which is a fundamental parameter in the decision-making process, is employed as the performance index. In order to evaluate the controllability, the cumulative pressure deviation from the set-point along with the minimum and maximum of pressure, which are reached by each boiler while supplying a specific profile, are measured. Considering the employed discrete variable methodology, the cumulative pressure deviation, which is the mean squared deviations of boiler vessel pressure from the instantaneous reference pressure (set-point value), is expressed as:

$$\sigma_P = \sum_{i=1}^{N_s} \sqrt{\frac{\left(p_{boiler,i} - p_{boiler,reference}\right)^2}{N_s}} \tag{21}$$

As given in Table 2, in the present study, the set point pressure ($p_{boiler,reference}$) is considered to be 15 bar. Apparently, low values of the latter index demonstrates that the boiler has met the desired pressure in a better manner. The fact that shows higher controllability and is thus desirable in the decision-making process.

Table 3 represents the cumulative average efficiency, which is achieved by each boiler while providing the mentioned steam demand profiles. As expected, by increasing the boilers' size, the corresponding efficiency enhances. However, apparently larger boiler size requires a higher initial investment, which should be taken into account in the decision-making process. The results provided in Table 3, for each steam request profile, facilitates choosing the smallest possible boiler while providing an acceptable efficiency. It can specifically be noted that, for some specific steam request profiles, beyond a certain size, using a larger boiler does

Table 1
Geometrical configurations of the considered boiler models.

Boiler model No.	Boiler radius [m]	Boiler length [m]	Furnace radius [m]	Number of tubes (2nd gas pass)	Net volume [m^3]	Metalic parts' weight [kg]	Heat transfer surface [m^2]	Water volume/heat transfer area [m]
1	0.50	2.00	0.25	30	1.06	463.7	12.57	0.0219
2	0.80	2.25	0.30	30	3.76	550.0	14.84	0.1006
3	1.00	3.70	0.35	34	9.95	1034.5	27.90	0.1484
4	1.25	4.50	0.40	36	19.51	1365.7	36.76	0.2303
5	1.48	6.00	0.50	40	36.10	2107.4	56.55	0.2734

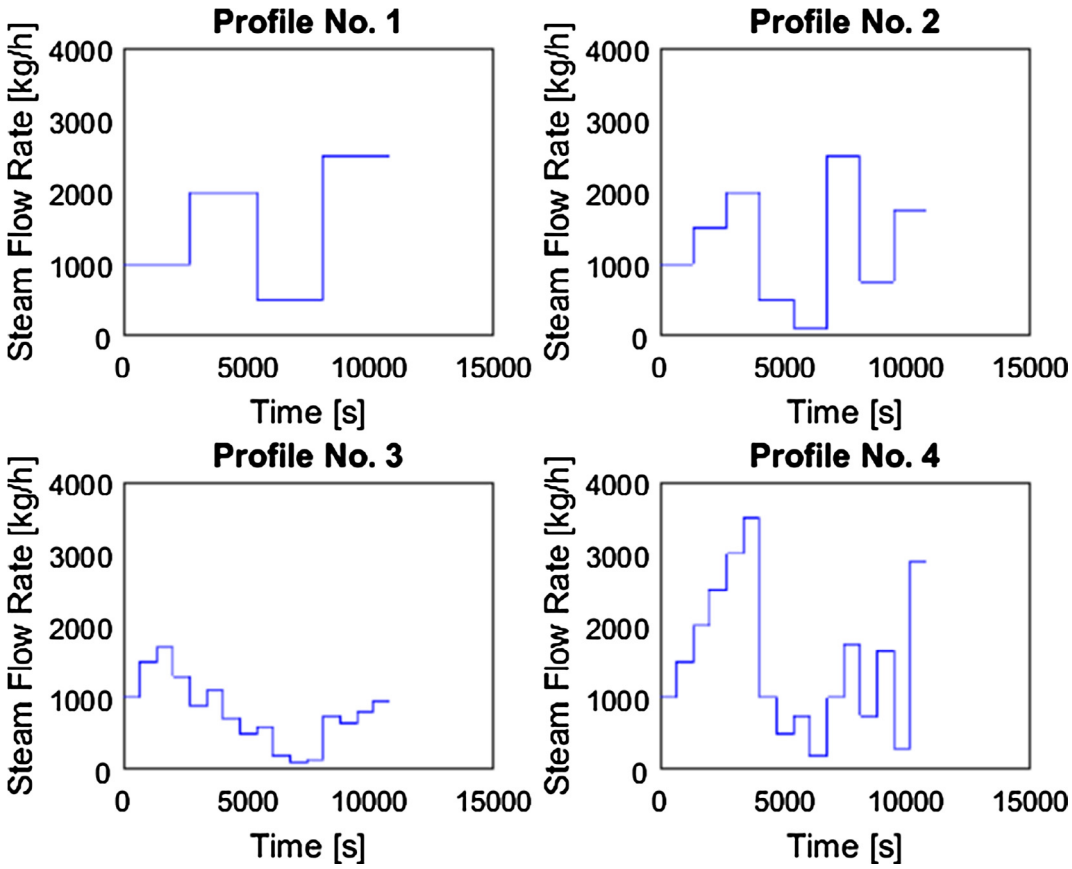

Fig. 4. Considered steam demand profiles.

Table 2
Considered operational limits of the boiler and the ambient conditions.

Parameters	Values
Steam pressure (set-point) [bar]	15
Maximum feed-water flow rate [kg/h]	3000
Feed-water temperature [°C]	80
Purge water flow rate [kg/h]	72
Maximum allowed fuel flow-rate [kg/h]	1000
Oxygen concentration at stack [%v]	3.0
Ambient temperature [°C]	20
Ambient pressure [bar]	1

not result in a notable increase in the efficiency. This can clearly be observed when simulating the 3rd steam demand profile, in which the difference between the efficiency obtained by using boiler No. 4 and No. 5 is less than 1%.

Nevertheless, as was previously discussed, controllability of the boiler should also be taken into account in the decision-making process. Therefore, the cumulative pressure deviations, which are determined for different boilers while addressing the considered load profiles, are represented in Table 4. For a specific profile, the value of the cumulative pressure deviation of a boiler is correlated to the damping provided by the water volume and metal parts which tend to stabilize the boiler conditions in presence of system variabilities. The controllability is also associated with the speed the boiler can adjust the fuel flow rate and satisfy the variations in the steam request. Thus, larger boilers have a greater thermal inertia (heat capacity), though are slower in adapting to the variation in the steam demand. Up to a certain size, the former effect (higher heat capacity) is dominant over the latter one by a large margin. Accordingly, as can be noticed in Table 4 for all of the considered profiles, increasing the size from boiler No. 1 to boiler No. 2 drastically decreases the cumulative pressure deviation. However, for larger sizes, these two effects become comparable and increasing the size of the boiler does not notably reduce the pressure deviation. The latter can be observed in the marginal difference between the cumulative pressure deviations achieved by boiler No. 4 and boiler No. 5 for all of the profiles.

Although, cumulative pressure deviation can be an effective index for evaluating the controllability of the boiler, further information regarding such deviations might be needed in order

Table 3
The determined cumulative average efficiencies obtained by different boiler models while imposing the considered steam demand profiles.

	Efficiency [–]				
	Boiler No. 1	Boiler No. 2	Boiler No. 3	Boiler No. 4	Boiler No. 5
Profile No. 1	0.723	0.744	0.828	0.846	0.860
Profile No. 2	0.724	0.745	0.826	0.843	0.856
Profile No. 3	0.753	0.765	0.824	0.835	0.842
Profile No. 4	0.725	0.746	0.831	0.848	0.862

Table 4
The determined cumulative pressure deviations obtained by different boiler models while imposing the considered steam demand profiles.

	Cumulative pressure deviation [bar]				
	Boiler No. 1	Boiler No. 2	Boiler No. 3	Boiler No. 4	Boiler No. 5
Profile No. 1	14.975	8.630	2.666	2.084	1.928
Profile No. 2	29.183	17.458	5.314	3.963	3.668
Profile No. 3	4.554	3.723	1.891	1.729	1.599
Profile No. 4	34.075	21.142	7.193	5.353	4.804

Table 5
The determined maximum and minimum pressure levels for different boilers models while imposing the considered steam demand profiles.

	Pressure level [bar]									
	Boiler No. 1		Boiler No. 2		Boiler No. 3		Boiler No. 4		Boiler No. 5	
	max	min	max	min	max	min	max	min	max	min
Profile No. 1	17.05	13.92	15.97	14.52	15.30	14.71	15.19	14.76	15.16	14.80
Profile No. 2	17.18	13.34	16.00	14.34	15.31	14.64	15.22	14.70	15.18	14.75
Profile No. 3	15.56	14.80	15.26	14.85	15.09	14.90	15.06	14.92	15.05	14.93
Profile No. 4	18.13	14.74	16.43	14.79	15.43	14.87	15.30	14.89	15.25	14.90

to verify the corresponding coherence with the requirement of the project. Hence, the maximum and minimum pressure levels reached by each boiler while supplying different steam demand profiles are reported in Table 5. Such values can be compared with the client's acceptable range of deviations from the set-point; thus, one can evaluate if a specific boiler can meet the client's project specifications. Furthermore, the amplitude of the pressure swing, in the form of cyclical stresses, can have an effect on the durability of boiler's structure and reduce its lifetime or increase its corresponding maintenance cost. The latter effect should also be taken into account in the sizing procedure of the boiler.

Similar to the cumulative pressure deviation results, the obtained minimum and maximum pressure values show that using larger boilers, beyond a certain size, does not result in a notable reduction in the pressure deviations. Hence, merging together the results presented in Tables 3 and 5, it can be observed that while addressing a highly variable demand profile (Profile No. 4), employing boiler No. 4 (with heat transfer surface of 36.76 m^2) instead of boiler No. 5 (with heat transfer surface of 56.55 m^2) leads to a reduction in efficiency of less than 2% while resulting in an insignificant change in pressure deviation's range. It was also shown that, for steam demand profiles with a limited variation

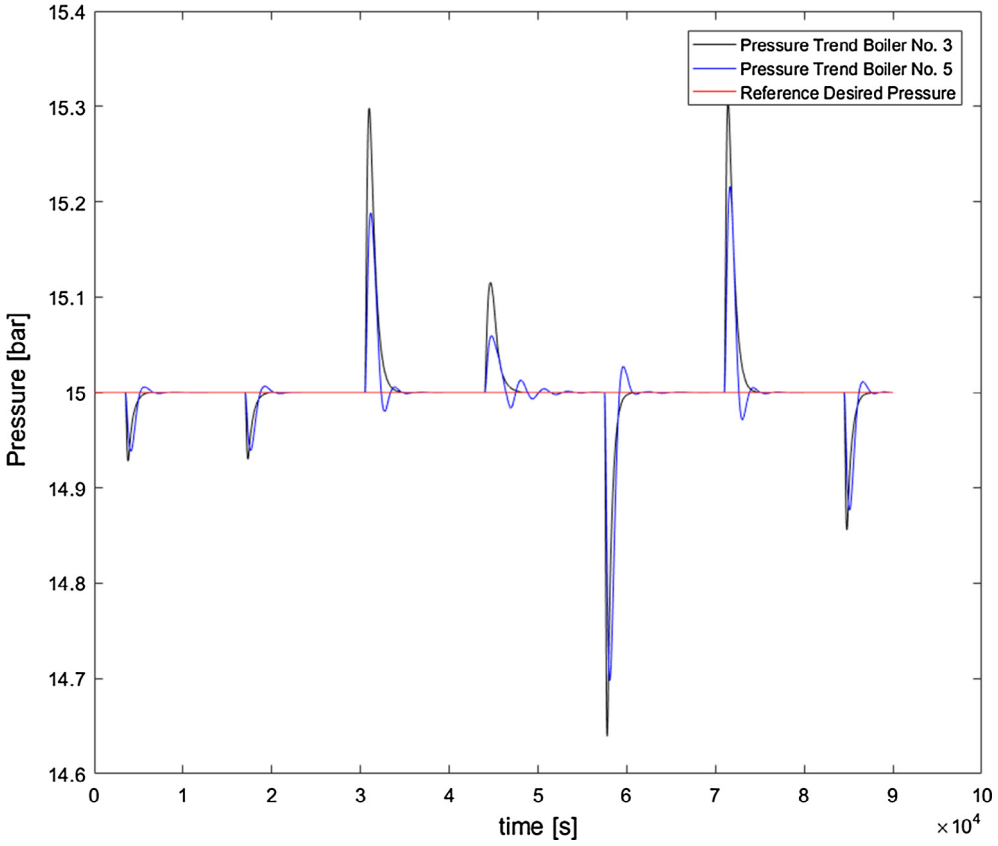

Fig. 5. Pressure trends of boiler No. 3 and boiler No. 5 compared with the reference while supplying the steam demand profile No. 2.

amplitude (profile No. 3), utilizing boiler No. 4 instead of boiler No. 5 leads to a negligible reduction (less than 1%) in the efficiency and controllability of the boiler. It was even demonstrated that, while meeting such profile, even employing boiler No. 3 (with heat transfer surface of 27.90 m^2) decreases the overall efficiency only by 1.8% while leading to a negligible increment in the amplitude of

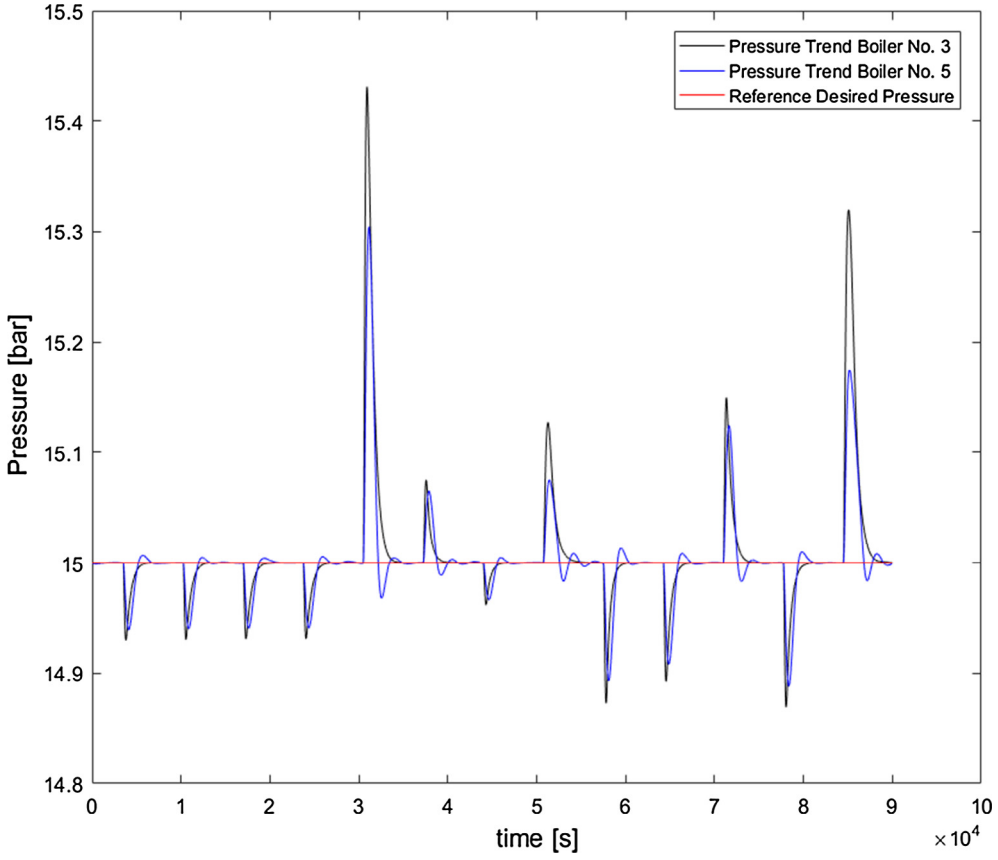

Fig. 6. Pressure trends of boiler No. 3 and boiler No. 5 compared with the reference while supplying the steam demand profile No. 4.

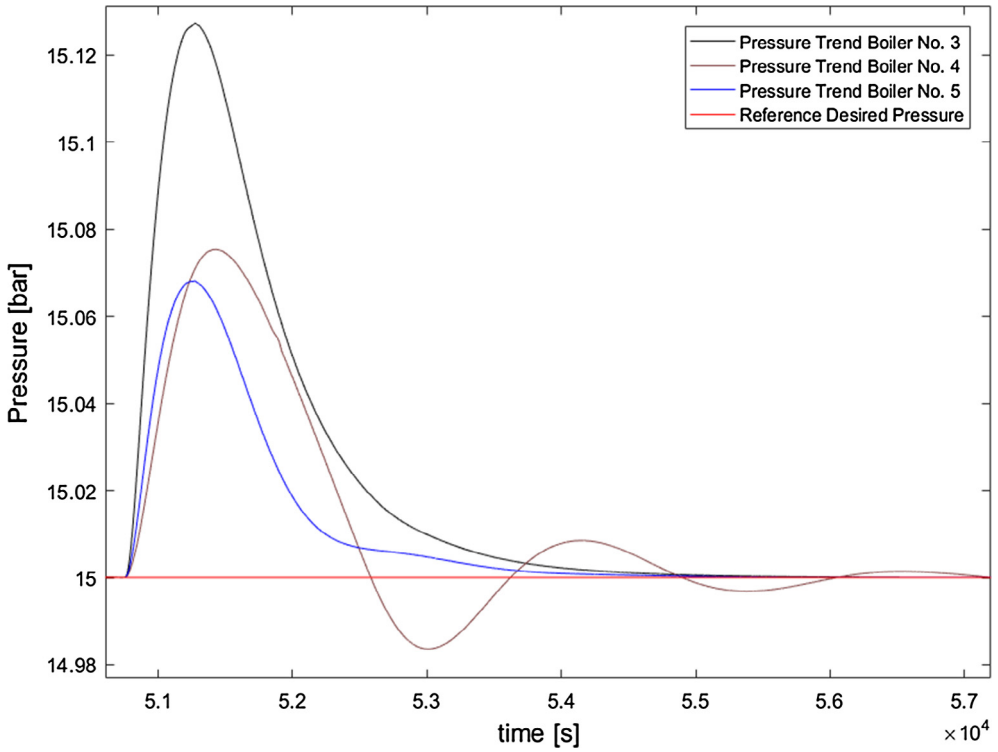

Fig. 7. A magnified representation of pressure trends of boiler No. 3 and boiler No. 4 and boiler No. 5 while supplying the steam demand profile No. 4.

pressure variations (from 0.67% to 1% with respect to the set point pressure). Thus, employing boiler No. 5 for such a profile is an oversized design that requires a notably higher investment while it does not result in any notable improvement in terms of efficiency or controllability. Accordingly, keeping in mind the customer's specifications and demand profile, one can evaluate utilizing smaller boilers in the sizing procedure, which can lead to a notable saving in the initial capital cost while assuring that the customer specifications are addressed.

In order to provide the reader with more detailed information regarding the effect of the size of the boiler on its corresponding controllability, graphical representation of pressure deviations are also provided. Fig. 5 demonstrates the pressures variations of boilers No. 3 and No. 5 while addressing the profile No. 2. Fig. 6 instead demonstrates the corresponding variation of the same boilers while meeting the demand of profile No. 4. As can be expected, these two figures demonstrate that faster load fluctuations result in higher pressure deviations. Fig. 7 is a magnified representation of pressure trends of boilers No. 3, No. 4, and No. 5, while supplying th e steam demand profile No. 4. The latter diagram illustrates the reduction of the pressure swing while increasing the size from boiler No. 3 to No. 5. It can also be observed that, although increasing the size of the boiler, and thus enhancing its thermal inertia, mitigates the peaks of pressure due to demand fluctuations, it does not affect the boiler's convergence time.

6. Conclusions

In the present study, a comprehensive dynamic model of fire-tube boilers was first developed and boiler configurations with notably different sizes were considered. PID tuning was next carried out for each boiler and operation of the boilers, while meeting four different steam demand profiles, was then simulated. The comparison of resulting average efficiencies revealed that, beyond a certain size, using a larger boiler does not lead to a significant increase in the performance. It was also confirmed that, as the PID controller is tuned for each configuration, utilizing a larger boiler does neither results in a notable benefit in terms of controllability. It was accordingly shown that, using a boiler with the heat transfer surface of 36.76 m^2 instead of one with the heat transfer surface of 56.55 m^2, results in a reduction in efficiency of less than 2% (less than 1% for demand profiles with limited variation amplitude). It was demonstrated that, for less variable demand profiles, using even a smaller boiler (with a heat transfer surface of 27.90 m^2) reduces the efficiency only by 1.8%. Therefore, smaller boilers can be employed without resulting in a significant decrease in performance indices while guaranteeing that the customer's steam demand specifications are met. Accordingly, the main contribution of the present study is enabling the decision maker to evaluate the possibility of utilizing smaller boilers, which clearly results in a notable saving in the required investment, by providing the average efficiency of boilers with different sizes while addressing various demand profiles. Furthermore, the pressure variation diagrams of the steam generated by different boiler sizes demonstrated that, if the PID controller is tuned for each configuration, utilizing smaller boilers, even while meeting notable variable steam demand profiles, does not lead to a significant deviation in the pressure of the produced steam. Thus, customer's steam quality concerns is not a notable constraint while evaluating the abovementioned saving opportunity.

Acknowledgment

The authors would like to acknowledge ICI Caldaie S.p.A for providing technical and financial support for this project.

Appendix A. Supplementary material

Supplementary data associated with this article can be found, in the online version, at https://doi.org/10.1016/j.applthermaleng.2017.12.082.

References

[1] K.N. Harris, Model Boilers and Boiler Making, TEE Publishing Limited, 2000.
[2] P. Colonna, H. van Putten, Dynamic modeling of steam power cycles. Part I-Modeling paradigm and validation, Appl. Therm. Eng. 27 (2007) 467–480.
[3] F.P. de Mello, Boiler models for system dynamic performance studies, IEEE Trans. Power Syst. 6 (1991) 66–74.
[4] E.J. Adam, J.L. Marchetti, Dynamic simulation of large boilers with natural recirculation, Comput. Chem. Eng. 23 (1999) 1031–1040.
[5] K.J. Åström, R.D. Bell, Drum-boiler dynamics, Automatica 36 (2000) 363–378.
[6] H. Kim, S. Choi, A model on water level dynamics in natural circulation drum-type boilers, Int. Commun. Heat Mass Transf. 32 (2005) 786–796.
[7] T. Yang, C. Cui, Y. Shen, Y. Lv, A novel denitration cost optimization system for power unit boilers, Appl. Therm. Eng. 96 (2016) 400–410.
[8] J.M. Blanco, L. Vazquez, F. Peña, Investigation on a new methodology for thermal power plant assessment through live diagnosis monitoring of selected process parameters; application to a case study, Energy 42 (2012) 170–180.
[9] S. Chandrasekharan, R.C. Panda, B. Natrajan Swaminathan, Dynamic analysis of the boiler drum of a coal-fired thermal power plant, Simulation 93 (2017) 995–1010.
[10] Y. Zhou, D. Wang, An improved coordinated control technology for coal-fired boiler-turbine plant based on flexible steam extraction system, Appl. Therm. Eng. 125 (2017) 1047–1060.
[11] L. Sun, D. Li, K.Y. Lee, Y. Xue, Control-oriented modeling and analysis of direct energy balance in coal-fired boiler-turbine unit, Control Eng. Practice 55 (2016) 38–55.
[12] H. Zhao, J. Shen, Y. Li, J. Bentsman, Coal-fired utility boiler modelling for advanced economical low-NOx combustion controller design, Control Eng. Pract. 58 (2017) 127–141.
[13] F. Rinaldi, B. Najafi, Temperature measurement in WTE boilers using suction pyrometers, Sensors (Switzerland) 13 (2013) 15633–15655.
[14] P.U. Sunil, J. Barve, P.S.V. Nataraj, Mathematical modeling, simulation and validation of a boiler drum: some investigations, Energy 126 (2017) 312–325.
[15] S. Kim, S. Choi, Dynamic simulation of the water-steam system in once-through boilers sub-critical power boiler case, Trans. Kor. Soc. Mech. Eng, B 41 (2017) 353–363.
[16] A. El-Guindy, S. Runzi, K. Michels, Optimizing drum-boiler water level control performance: a practical approach, in: 2014 IEEE Conference on Control Applications, CCA 2014, 2014, pp. 1675–1680.
[17] E. Oko, M. Wang, J. Zhang, Neural network approach for predicting drum pressure and level in coal-fired subcritical power plant, Fuel 151 (2015) 139–145.
[18] K. Sørensen, Modelling and simulating fire tube boiler performance, in: Proceedings from SIMS 2003-44th Conference on Simulation and Modeling on September 18-19, Session 2b, Lecture 7, 2003 in Västers.
[19] B.J. Huang, P.Y. Ko, System dynamics model of fire-tube shell boiler, J. Dynam. Syst., Measure. Control, Trans. ASME 116 (1994) 745–754.
[20] H. Rusinowski, W. Stanek, Neural modelling of steam boilers, Energy Convers. Manage. 48 (2007) 2802–2809.
[21] M. Manivannan, B. Najafi, F. Rinaldi, Machine learning-based short-term prediction of air-conditioning load through smart meter analytics, Energies 10 (2017) 1905.
[22] P.J. Coelho, P.A. Novo, M.G. Carvalho, Modelling of a utility boiler using parallel computing, J. Supercomput. 13 (1999) 211–232.
[23] C.K. Westbrook, Y. Mizobuchi, T.J. Poinsot, P.J. Smith, J. Warnatz, Computational combustion, Proc. Combust. Inst. 30 (2005) 125–157.
[24] A. Gómez, N. Fueyo, L.I. Díez, Modelling and simulation of fluid flow and heat transfer in the convective zone of a power-generation boiler, Appl. Therm. Eng. 28 (2008) 532–546.
[25] M. Pezo, V.D. Stevanovic, Z. Stevanovic, A two-dimensional model of the kettle reboiler shell side thermal-hydraulics, Int. J. Heat Mass Transf. 49 (2006) 1214–1224.
[26] A. Habibi, B. Merci, G.J. Heynderickx, Impact of radiation models in CFD simulations of steam cracking furnaces, Comput. Chem. Eng. 31 (2007) 1389–1406.
[27] B. Najafi, H. Najafi, M.D. Idalik, Computational fluid dynamics investigation and multi-objective optimization of an engine air-cooling system using a genetic algorithm, Proc. Inst. Mech. Eng., Part C: J. Mech. Eng. Sci. 225 (2011) 1389–1398.
[28] F.J. Gutiérrez Ortiz, Modeling of fire-tube boilers, Appl. Therm. Eng. 31 (2011) 3463–3478.
[29] A. Haghighat Mamaghani, B. Najafi, A. Casalegno, F. Rinaldi, Long-term economic analysis and optimization of an HT-PEM fuel cell based micro combined heat and power plant, Appl. Therm. Eng. 99 (2016) 1201–1211.
[30] A. Haghighat Mamaghani, B. Najafi, A. Casalegno, F. Rinaldi, Predictive modelling and adaptive long-term performance optimization of an HT-PEM fuel cell based micro combined heat and power (CHP) plant, Appl. Energy 192 (2017) 519–529.

[31] T. Selleri, B. Najafi, F. Rinaldi, G. Colombo, Mathematical modeling and multi-objective optimization of a mini-channel heat exchanger via genetic algorithm, J. Therm. Sci. Eng. Applicat. 5 (2013).
[32] M. Aminyavari, A.H. Mamaghani, A. Shirazi, B. Najafi, F. Rinaldi, Exergetic, economic, and environmental evaluations and multi-objective optimization of an internal-reforming SOFC-gas turbine cycle coupled with a Rankine cycle, Appl. Therm. Eng. 108 (2016) 833–846.
[33] M.E. Flynn, M.J. O'Malley, A drum boiler model for long term power system dynamic simulation, IEEE Trans. Power Syst. 14 (1999) 209–217.
[34] Y.A. Çengel, Heat Transfer: A Practical Approach, seond ed., McGraw-Hill, Boston, 2003.
[35] H.C. Hottel, A.F. Sarofim, Radiative Transfer, McGraw-Hill, 1967.
[36] E. Talmor, Combustion Hot Spot Analysis for Fired Process Heaters, 1982.
[37] M.G. Cooper, Heat flow rates in saturated nucleate pool boiling – a wide-ranging correlation using reduced properties, Adv. Heat Transf. 16 (1984) 158–239.
[38] K. Groves, A. Serrani, Modeling and nonlinear control of a single-link flexible joint manipulator, Appendices, Ohio State University, 2004.